2011 American Control Conference
on O'Farrell Street, San Francisco, CA, USA
June 29 - July 01, 2011

Spacecraft Reorientation in Presence of Attitude Constraints via Logarithmic Barrier Potentials

Unsik Lee and Mehran Mesbahi

***Abstract*— This paper proposes a methodology–based on convex navigation functions– for three-axis attitude reorientation for a rigid body spacecraft in presence of multiple constraints. In this direction, two types of attitude constrained zones are first defined, namely, the attitude forbidden and mandatory zones. The paper then utilizes a convex parameterization of forbidden and mandatory zones for constructing a logarithmic barrier potential function that is subsequently used for the synthesis of the attitude control laws. The feasible controller– which uses the feedback of the unit quaternions in the context of the proposed methodology– is then implemented using a modified integrator back-stepping method in order to compromise the actuator saturations. The paper concludes with a set of simulation results in order to evaluate the effectiveness, and demonstrate the viability, of the proposed methodology.**

I. INTRODUCTION

One of the key technologies for spacecraft autonomy is the execution of large angle reorientations in presence of constraints. For example, spacecraft involved in science missions are often equipped with sensitive payloads, such as infrared telescopes or interferometers, that require re-targeting while avoiding direct exposure to the sunlight or other bright objects. Planning a re-orientation in presence of attitude constraints is of paramount importance in such science applications; it also poses a particularly challenging computational task for the spacecraft guidance, navigation, and control subsystem. This is mainly due to the fact that removing the constrained zones from the rotational configuration space of the spacecraft results in a *nonconvex* region. The spacecraft reorientation problem in the absence of attitude constraints has been comprehensively addressed in the literature; see for example [8], [14]. On the contrary, the attitude reorientation problem in presence of attitude constraints has been examined in only a few research works. For example, McInnes considered and implemented maneuver planning in presence of attitude constraints via an artificial potential function in [1], [3]. However, due to the use of Euler angles in McInnes' works, the possibility of having singularities during reorientation maneuvers could not be ruled out. Another set of approaches to constrained attitude control which rely on geometric relations between direction of instrument's boresight and the bright celestial object to be avoided, has been introduced by Spindler[4], Hablani[5], and Frakes *et al.*[6]. In these works, a feasible attitude trajectory is determined prior to the reorientation maneuver. However, these approaches have the disadvantage of not being extendible to more complex situations, involving multiple celestial constraints often encountered in actual space missions. Over the last decade, alternative approaches using randomized algorithms have been proposed by Frazzoli[7], Kornfeld[11], and Cui[9]. The randomization-based approaches have an advantage in terms of their ability in handling distinct classes of constraints, with provable–albeit probabilistic–convergence properties. The randomized algorithms, however, have limitations in terms of their on-board implementation and might result in execution times that, depending on the types of constraints and initial and final attitudes, can be of exponential order. In this paper, we develop a potential function based method that builds on the recent convex parameterization of attitude constraint in quaternion space proposed by Kim and Mesbahi [12], [13], which in turn builds on the constraints representation discussed in [10]. The advantage of the proposed approach hinges upon the fact that the logarithmic barrier potential function used for constructing the corresponding control law is smooth and strictly *convex*. This in turn implies that the proposed methodology can handle large number of forbidden and mandatory zones simultaneously, while guaranteeing computational tractability and convergence. Then, a feedback controller is implemented based on the convex logarithmic barrier potential function. The modified back-steeping method has been used to derive the controller following the negative gradient of the proposed convex potential while attenuating the excess and sharp controls originally embedded in the regular back-stepping method.

The rest of the paper is organized as follows. §II reviews the mathematical models of rigid-body kinematics and dynamics using quaternions. In §III, we proceed to define and parameterize two classes of attitude constraints for constructing a logarithmic barrier potential function. A control design technique for the constrained attitude maneuver is then presented in §IV. This is subsequently followed by simulation results for various scenarios in §V. Conclusions and possible future extensions of this work are detailed in §VI.

II. BACKGROUND

The attitude dynamics of a rigid body spacecraft with fully actuated body-fixed torquing devices can be described by the following system of kinematic and dynamic equations [2],

$$\dot{\boldsymbol{q}}(t) = \frac{1}{2}\boldsymbol{q}(t) \otimes \widetilde{\boldsymbol{\omega}}(t), \tag{1}$$

$$J\dot{\vec{\omega}}(t) = R(\vec{\omega})\, J\vec{\omega}(t) + \vec{u}(t), \tag{2}$$

where $\boldsymbol{q}(t)$ is the unit quaternion representing the attitude of the rigid body, $\widetilde{\boldsymbol{\omega}}(t) = [\vec{\omega}^T\ 0]^T_{4\times 1}$, and $\vec{\omega}(t) \in \mathbb{R}^3$ denotes the angular velocity of the spacecraft in the body frame, $J = \mathbf{Diag}(J_1,\ J_2,\ J_3)$ denotes the body frame aligned inertia matrix of the spacecraft, $\vec{u}(t) \in \mathbb{R}^3$ represents the control torque about the body axes, and $R(\vec{\omega})$ denotes the cross product operator in matrix form associated with $\vec{\omega}$. A unit quaternion representing a rigid body attitude is defined as $\boldsymbol{q} = [\vec{q}^T\ q_0]^T \in \mathbb{R}^4$, where $\vec{q} = \widehat{\mathbf{n}}\,\sin(\frac{\phi}{2}) \in \mathbb{R}^3$ denotes the "vector part" of the quaternion and $q_0 = \cos(\frac{\phi}{2}) \in \mathbb{R}$ denotes the "scalar part" of the quaternion $\boldsymbol{q}$, with $\widehat{\mathbf{n}}$ and ϕ referring to, respectively, the Euler axis and the rotation angle about this axis corresponding to the rigid body orientation. The unit quaternion is globally non-singular but possesses a sign obscureness, which stems from the fact that $-\boldsymbol{q}$ represents the same rotation as $\boldsymbol{q}$. We avoid the situation that the sign of the quaternion changes instantaneously by keeping its value satisfying its kinematic equation. In Eq. (1), as

The authors are with the Department of Aeronautics and Astronautics, University of Washington, Seattle, WA 98195-2400.

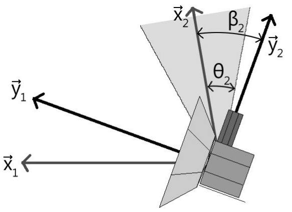

Fig. 1. An attitude forbidden zone associated with an instrument boresight vector $\vec{y}_2$.

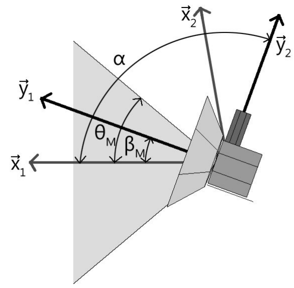

Fig. 2. An attitude mandatory zone associated with an instrument boresight vector $\vec{y}_1$.

well as in subsequent sections, the product "$\otimes$" refers to quaternion multiplication defined by

$$\boldsymbol{\alpha} \otimes \boldsymbol{\beta} = \begin{bmatrix} \alpha_0\vec{\beta} + \beta_0\vec{\alpha} + \vec{\alpha} \times \vec{\beta} \\ \alpha_0\beta_0 - \vec{\alpha}^T\vec{\beta} \end{bmatrix},$$

where $\vec{\alpha}$, $\vec{\beta}$, α_0, and β_0 are, respectively, the vector and scalar parts of unit quaternions $\boldsymbol{\alpha}$ and $\boldsymbol{\beta}$. Another quaternion operation is the "quaternion transpose" defined as $\boldsymbol{q}^\star = [\ -\vec{q}^T \quad q_0\ ]^T$ which facilitates the judicious definition for "attitude error" between two orientations in unit quaternions $\boldsymbol{\alpha}$, $\boldsymbol{\beta}$ via $\boldsymbol{\alpha}^\star \otimes \boldsymbol{\beta}$. In what follows, we will assume that all external disturbances on the spacecraft are negligible.

III. Problem Statement

In this section, we first define three types of attitude constraint zones that will be the focus of our discussion in this paper.

1. **Attitude Forbidden Zone:** A set of spacecraft orientations, such as the set of attitudes that lead sensitive on-board instruments have direct exposure to a given celestial objects such as the sun, is considered as an attitude forbidden zone. Multiple constraint zones can be specified with respect to a single instrument boresight vector.
2. **Attitude Mandatory Zone:** The set of spacecraft orientations, such as the set of attitudes that lead certain on-board instruments point toward specified objects, e.g., pointing a high gain antenna to a ground station, is considered as an attitude mandatory zone. The attitude mandatory zones for each instrument should be non-conflicting.
3. **Attitude Permissible Zone**: The set of spacecraft orientation is considered to be in the attitude permissible zone when it is at the intersection of the complements of attitude forbidden zones on one hand, and the attitude mandatory zones, on the other.

Using unit quaternion representation for spacecraft orientation, the above three constraint zones can be parameterized in the form of quadratic inequalities shown below; for more details see [12].

Proposition 1: Let the unit quaternion $\boldsymbol{q} \in \mathcal{U}_q$ describe the attitude of the spacecraft whose boresight vector $\vec{y}_j$ for the jth instrument, e.g., a telescope, lies outside of the attitude forbidden zone, i.e., $\beta_2 > \theta_2$ in Fig.1. Then the subset $\mathcal{Q}_{F_j} \subseteq \mathcal{U}_q$ satisfying the above condition can be represented as,

$$\mathcal{Q}_{F_j} = \{\, \boldsymbol{q} \subseteq \mathcal{U}_q \mid \boldsymbol{q}^T M_i^j(\theta_i)\boldsymbol{q} < 0\}, \tag{3}$$

with

$$M_i^j(\theta_i) = \begin{bmatrix} A_i^j & b_i^j \\ b_i^{jT} & d_i^j \end{bmatrix}, \tag{4}$$

where $A_i^j = \vec{x}_i\vec{y}_j^{\,T} + \vec{y}_j\vec{x}_i^T - \left(\vec{x}_i^T\vec{y}_j + \cos\theta_i\right)\mathbf{I}_3$, $b_i^j = \vec{x}_i \times \vec{y}_j$, and $d_i^j = \vec{x}_i^T\vec{y}_j - \cos\theta_i$, with $i = 1, 2, \cdots n$, $j = 1, 2, \cdots m$.

The notation used above needs further elaboration. The index n represents the number of constraint zones associated with the jth on-board instrument; the index m on the other hand, is the total number of instruments. Moreover, $\vec{x}_i$ denotes the unit vector (specified in the inertial frame) for the ith constrained object to be avoided, while $\vec{y}_j$ indicates the unit vector (in the body frame) representing the boresight direction of the jth sensitive equipment on the spacecraft. The angle θ_i is the angle about the direction of the ith constrained object specified by $\vec{x}_i$. Without loss of generality, the domain of the angle θ_i, for all i, is restricted to be $(0, \pi]$. We note that the attitude forbidden zone is generally defined not only with respect to the number of sensitive instrument on-board m, but also with respect to the number of constrained objects n.

Proposition 2: The set $\mathcal{Q}_M \subseteq \mathcal{U}_q$ representing possible attitude of the spacecraft, about which the boresight vector of an on-board instrument, e.g., an antenna, lies inside the attitude mandatory zone, i.e., $\beta_M < \theta_M$ in Fig. 2, can be represented as,

$$\mathcal{Q}_M = \{\, \boldsymbol{q} \in \mathcal{U}_q \mid \boldsymbol{q}^T M_M(\theta_M)\boldsymbol{q} > 0\,\}, \tag{5}$$

where $M_M(\theta_M)$ and θ_M are defined analogously to Proposition 1; the latter is the angle with respect to the boresight vector of an on-board instrument that should stay in the attitude mandatory zone.

Note that we have considered the case where only one attitude mandatory zone is present; this is without loss of generality, as if multiple mandatory zones are present, then only the set defined by their intersection can be considered.

Let us now provide a representation for the **Attitude Permissible Zone**. The subset $\mathcal{Q}_P$, parameterizing the attitude of the spacecraft satisfying the attitude mandatory zones, as well as avoiding the attitude forbidden zones, is given by,

$$\mathcal{Q}_p = \left\{ \boldsymbol{q} \in \mathcal{U}_q \mid -\boldsymbol{q}^T M_i^j \boldsymbol{q} > 0 \text{ and } \boldsymbol{q}^T M_M \boldsymbol{q} > 0 \right\}$$
$$\text{for } i = 1, 2, \ldots n,\ j = 1, 2, \ldots m.$$

Fig. 3 shows three types of attitude zones represented on the celestial sphere defined for two instruments boresight vectors.

A. Logarithmic barrier potential

We now discuss observations that will be subsequently used for the convex parameterization of the forbidden and mandatory zones and their embedding in a potential function.

Proposition 3: Let $M(\theta)$ be the matrix used to represent the attitude forbidden zones in Eq. (4). Then for all $\theta_i \in (0, \pi]$ and $\boldsymbol{q} \subseteq \mathcal{U}_q$, one has

$$-2 < \lambda_{\min}(M(\theta)) \leq \boldsymbol{q}^T M(\theta))\boldsymbol{q} \leq \lambda_{\max}(M(\theta)) < 2. \tag{6}$$

Proof: From Eq. (4), the symmetric matrix $M(\theta)$ can be written as

$$M(\theta) = P(\theta) - \cos\theta_i \mathbf{I}_4 \tag{7}$$

where

$$P(\theta) = \begin{bmatrix} \vec{x}_i\vec{y}^T + \vec{y}\vec{x}_i^T - (\vec{x}_i^T\vec{y})\mathbf{I}_3 & \vec{x}_i \times \vec{y} \\ \left(\vec{x}_i \times \vec{y}\right)^T & \vec{x}_i^T\vec{y} \end{bmatrix}.$$

Since vectors x_i and y are unit vectors, $P^TP = \mathbf{I}_4$. Thus,

$$Pv = \lambda_p v,\ P^TPv = \lambda_p Pv,\ \left(\mathbf{I}_4 - \lambda_p^2\mathbf{I}_4\right)v = 0,$$

where λ_p is an eigenvalue of P and v is the corresponding eigenvector. The eigenvalues of P, on the other hand, are given as $\lambda_p = -1,\ -1,\ 1,\ 1$. Note that from Eq. (7), eigenvalues of

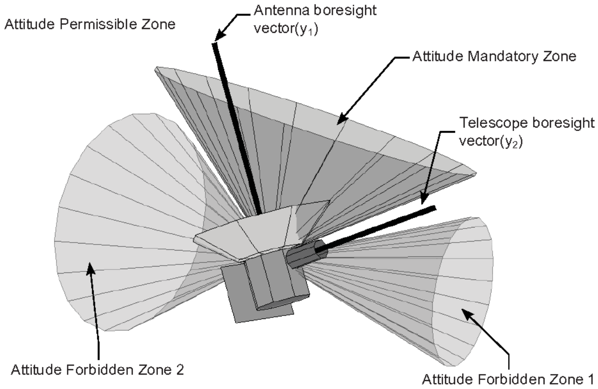

Fig. 3. 3 types of zones drawn on celestial space

the matrix $M(\theta)$ are shifted from λ_p depending on $\cos\theta_i$, which assume values between -1 and 1. Thus, in view of the fact that $\|\boldsymbol{q}(t)\| = 1$, Eq. (6) follows. ■

Proposition 4: Let $M(\theta)$ be the matrix used to represent the **Attitude Forbidden Zones** in Eq. (4) and consider the quaternion subset $\mathcal{Q}_{F_j} \subseteq \mathcal{U}_q$ defined in Proposition 1 specified as

$$\mathcal{Q}_{F_j} = \{\, \boldsymbol{q} \in \mathcal{U}_q \mid \boldsymbol{q}^T M(\theta)\boldsymbol{q} < 0 \,\}.$$

Then this set can be represented as the convex set [13],

$$\mathcal{Q}^{'}_{F_j} = \{\, \boldsymbol{q} \in \mathcal{U}_q \mid \boldsymbol{q}^T \widetilde{M}(\theta)\boldsymbol{q} < 2 \,\},$$

where $\widetilde{M}(\theta) \in \mathbb{S}^n_{++}$.

Proof: From Proposition 3, it follows that,

$$\begin{aligned}
&\lambda_{\min}(M(\theta)) \le \boldsymbol{q}^T M(\theta)\boldsymbol{q} < 0,\\
&\lambda_{\min}(M(\theta)) + 2 \le \boldsymbol{q}^T M(\theta)\boldsymbol{q} + 2\boldsymbol{q}^T\boldsymbol{q} < 2,\\
&\lambda_{\min}(M(\theta)) + 2 \le \boldsymbol{q}^T (M(\theta) + 2\mathbf{I})\boldsymbol{q} < 2,\\
&0 < \lambda_{\min}(M(\theta)) + 2 \le \boldsymbol{q}^T \widetilde{M}(\theta)\boldsymbol{q} < 2,\\
&0 < \boldsymbol{q}^T \widetilde{M}(\theta)\boldsymbol{q} < 2,
\end{aligned}$$

where $\boldsymbol{q}^T\boldsymbol{q} = 1$ and $\widetilde{M}(\theta) \in \mathbb{S}^n_{++}$. Therefore the subsets $\mathcal{Q}_{F_j}$ and $\mathcal{Q}^{'}_{F_j}$ above represent the same convex set. ■

Proposition 5: Analogous to Proposition 4, let $M_M(\theta) \in \mathbb{S}^4$ be the matrix used to define Eq. (5). Then the subset $\mathcal{Q}_M \subseteq \mathcal{U}_q$ specifying the **Attitude Mandatory Zone**,

$$\mathcal{Q}_M = \{\, \boldsymbol{q} \in \mathcal{U}_q \mid \boldsymbol{q}^T M_M(\theta)\boldsymbol{q} > 0 \,\},$$

can be represented as a convex set

$$\mathcal{Q}^{'}_M = \{\, \boldsymbol{q} \in \mathcal{U}_q \mid \boldsymbol{q}^T \widetilde{M}_M(\theta)\boldsymbol{q} < 2 \,\},$$

where $\widetilde{M}_M(\theta) \in \mathbb{S}^n_{++}$.

Proof: The proof follows by observing the following inequalities,

$$\begin{aligned}
&-2 < \boldsymbol{q}^T M_M(\theta)\boldsymbol{q} - 2 \le \lambda_{\max}(M(\theta)) - 2,\\
&-2 < -\boldsymbol{q}^T \widetilde{M}_M(\theta)\boldsymbol{q} \le \lambda_{\max}(M(\theta)) - 2,\\
&-\lambda_{\max}(M(\theta)) + 2 \le \boldsymbol{q}^T \widetilde{M}_M(\theta)\boldsymbol{q} < 2,
\end{aligned}$$

where $\boldsymbol{q}^T\boldsymbol{q} = 1$ and $\widetilde{M}_M \in \mathbb{S}^n_{++}$. Hence, the two subsets $\mathcal{Q}_M$ and $\mathcal{Q}^{'}_M$ above represent the same convex set. ■

In order to embed the convex parameterization of the forbidden and mandatory zones into a potential function, we consider the logarithmic barrier function $V_q : \mathcal{D}_q \to \mathbb{R}$,

$$V_q(\boldsymbol{q}) = \|\boldsymbol{q}_r^\star \otimes \boldsymbol{q} - \boldsymbol{q}_{\mathrm{I}}\|^2 \Big[\Big(\sum_{j=1}^{m}\sum_{i=1}^{n} -k_1 \log(-\frac{\boldsymbol{q}^T M_i^j \boldsymbol{q}}{2})\Big) - k_2 \log(\frac{\boldsymbol{q}^T M_M \boldsymbol{q}}{2})\Big], \tag{8}$$

where

$$\mathcal{D}_q \subseteq \mathcal{Q}_p = \Big\{ \boldsymbol{q} \in \mathcal{U}_q \mid -\boldsymbol{q}^T M_i^j \boldsymbol{q} > 0 \text{ and } \boldsymbol{q}^T M_M \boldsymbol{q} > 0 \Big\}$$
$$\text{for } i = 1, 2, \ldots n,\ j = 1, 2, \ldots m,$$

k_1 and k_2 are positive weighting parameters for the attitude forbidden and mandatory zones, respectively, and $\boldsymbol{q}_r$ is the desired destination attitude. We note that the notational dependencies of the matrices M_i^j and M_M on the angle θ_i have been suppressed above; we will continue to use this abbreviated notation in the reminder of our discussion.

Proposition 6: The potential function V_q in Eq. (8) is smooth and strictly convex for all $\boldsymbol{q} \in \mathcal{D}_q$ and has a global minimum at $\boldsymbol{q}_r \in \mathcal{D}_q$.

Proof: We will show that V_q in Eq. (8) meets the following three conditions:

1) $V_q(\boldsymbol{q}_r) = 0$,
2) $V_q(\boldsymbol{q}) > 0$, for all $\boldsymbol{q} \in \mathcal{U}_q \backslash \{q_r\}$,
3) $\nabla^2 V_q(\boldsymbol{q})$ is positive definite for all $\boldsymbol{q} \in \mathcal{U}_q$.

First note that that $V_q(\boldsymbol{q}_r) = 0$ since $\boldsymbol{q}_r^\star \otimes \boldsymbol{q}_r = \boldsymbol{q}_{\mathrm{I}}$. From Eq. (6) and for all $\boldsymbol{q} \in \mathcal{D}_q$, the following inequalities are valid,

$$0 < -\frac{\boldsymbol{q}^T M_i^j \boldsymbol{q}}{2} < 1 \quad \text{and} \quad 0 < \frac{\boldsymbol{q}^T M_M \boldsymbol{q}}{2} < 1,$$

and hence the negative logarithm function Eq. (8) is always positive and for all $\boldsymbol{q} \in \mathcal{D}_q$,

$$\sum_{i=1}^{n} -\log(-\frac{\boldsymbol{q}^T M_i^j \boldsymbol{q}}{2}) > 0 \quad \text{and} \quad -\log(\frac{\boldsymbol{q}^T M_M \boldsymbol{q}}{2}) > 0.$$

Hence $V_q(\boldsymbol{q}) > 0$ for all $\boldsymbol{q} \in \mathcal{D}_q \backslash \{\boldsymbol{q}_r\}$. The third condition can be shown by first swapping the quaternion quadratic terms $-\boldsymbol{q}^T M_i^j \boldsymbol{q}$ and $\boldsymbol{q}^T M_M \boldsymbol{q}$ for the following equivalent terms as:

$$\begin{aligned}
-\boldsymbol{q}^T M_i^j \boldsymbol{q} &> 0,\\
-\boldsymbol{q}^T M_i^j \boldsymbol{q} + \beta_1 - \beta_1 &> 0,\\
\boldsymbol{q}^T \widetilde{M}_i^j \boldsymbol{q} - \beta_1 &> 0,
\end{aligned} \tag{9}$$

where β_1 is defined as $-\lambda_{\max}(M_i^j) + \beta_1 > 0$ so that $\widetilde{M}_i^j$ is a positive definite matrix, and

$$\begin{aligned}
\boldsymbol{q}^T M_M \boldsymbol{q} &> 0,\\
\boldsymbol{q}^T M_M \boldsymbol{q} + \beta_2 - \beta_2 &> 0,\\
\boldsymbol{q}^T \widetilde{M}_M \boldsymbol{q} - \beta_2 &> 0,
\end{aligned} \tag{10}$$

where β_2 is defined as $\lambda_{\min}(M_M) + \beta_2 > 0$ such that $\widetilde{M}_M$ is a positive definite matrix. Now the potential function (8) assumes the form

$$V_q(\boldsymbol{q}) = \|\boldsymbol{q}_r^\star \otimes \boldsymbol{q} - \boldsymbol{q}_{\mathrm{I}}\|^2 \Big[\Big(\sum_{j=1}^{m}\sum_{i=1}^{n} -k_1 \log(\frac{\boldsymbol{q}^T \widetilde{M}_i^j \boldsymbol{q} - \beta_1}{2})\Big) - k_2 \log(\frac{\boldsymbol{q}^T \widetilde{M}_M \boldsymbol{q} - \beta_2}{2})\Big].$$

The above expression for the potential function comprises of linear combinations of logarithmic functions. Since the summation of strictly convex functions is strictly convex, it suffices to analyze one of the terms in more detail. In this venue, consider the term,

$$V_q(\boldsymbol{q}) = \|\boldsymbol{q}_r^* \otimes \boldsymbol{q} - \boldsymbol{q}_{\mathbf{I}}\|^2 \left(\sum_i -k \log\left(\frac{\boldsymbol{q}^T \widetilde{M}_i^j \boldsymbol{q} - \beta_1}{2}\right)\right)$$

for some index j. Now, the gradient of V_q is calculated as

$$\nabla \boldsymbol{V}_q = \frac{\partial}{\partial \boldsymbol{q}} \|\boldsymbol{q}_r^\star \otimes \boldsymbol{q} - \boldsymbol{q}_{\mathbf{I}}\|^2 \left(\sum_i -k \log\left(\frac{\boldsymbol{q}^T \widetilde{M}_i^j \boldsymbol{q} - \beta_1}{2}\right)\right) + \|\boldsymbol{q}_r^\star \otimes \boldsymbol{q} - \boldsymbol{q}_{\mathbf{I}}\|^2 \left(\sum_i \frac{-2k}{\boldsymbol{q}^T \widetilde{M}_i^j \boldsymbol{q} - \beta_1} \boldsymbol{q}^T \widetilde{M}_i^j \right).$$

From the fact that $\frac{\partial}{\partial \boldsymbol{q}}(\|\boldsymbol{q}_r^\star \otimes \boldsymbol{q} - \boldsymbol{q}_{\mathbf{I}}\|^2) = -2\boldsymbol{q}_r^T$, $\frac{\partial^2}{\partial \boldsymbol{q}^2}(\|\boldsymbol{q}_r^\star \otimes \boldsymbol{q} - \boldsymbol{q}_{\mathbf{I}}\|^2) = 0_{4\times4}$, and $\|\boldsymbol{q}_r^\star \otimes \boldsymbol{q} - \boldsymbol{q}_{\mathbf{I}}\|^2 = 2 - 2\boldsymbol{q}_r^T \boldsymbol{q}$, the Hessian $\nabla^2 V_q$ is given as

$$\begin{aligned}\nabla^2 V_q = \sum_i \Bigg\{ & \frac{4k}{\boldsymbol{q}^T \widetilde{M}_i^j \boldsymbol{q} - \beta_1} \boldsymbol{q}_r \boldsymbol{q}^T \widetilde{M}_i^j + \frac{4k}{\boldsymbol{q}^T \widetilde{M}_i^j \boldsymbol{q} - \beta_1} \widetilde{M}_i^j \boldsymbol{q} \boldsymbol{q}_r^T \\ & + (2 - 2\boldsymbol{q}_r^T \boldsymbol{q}) \frac{4k}{(\boldsymbol{q}^T \widetilde{M}_i^j \boldsymbol{q} - \beta_1)^2} (\boldsymbol{q}^T \widetilde{M}_i^j)^T \boldsymbol{q}^T \widetilde{M}_i^j \\ & - (2 - 2\boldsymbol{q}_r^T \boldsymbol{q}) \frac{2k}{\boldsymbol{q}^T \widetilde{M}_i^j \boldsymbol{q} - \beta_1} \widetilde{M}_i^j \Bigg\}.\end{aligned}$$

Multiplying the last identity by $\boldsymbol{q}^T$ and $\boldsymbol{q}$ from left and right now yields

$$\boldsymbol{q}^T \nabla^2 V_q \boldsymbol{q} = \sum_i \gamma \left\{ (\boldsymbol{q}^T \widetilde{M}_i^j \boldsymbol{q} - 3\beta_1) \boldsymbol{q}_r^T \boldsymbol{q} + (\boldsymbol{q}^T \widetilde{M}_i^j \boldsymbol{q} + \beta_1) \right\},$$

where $\gamma = \frac{4k\boldsymbol{q}^\gamma \widetilde{M}_i^j \boldsymbol{q}}{(\boldsymbol{q}^T \widetilde{M}_i^j \boldsymbol{q} - \beta_1)^2}$, which is always a positive value as $\boldsymbol{q}^T \widetilde{M}_i^j \boldsymbol{q} + \beta_1 > 0$ for all $\boldsymbol{q} \in \mathcal{D}_q$ and $\beta_1 > 0$. The above equation is a linear function of $\boldsymbol{q}_r^T \boldsymbol{q}$. Since $\boldsymbol{q}_r^T \boldsymbol{q} \in [-1, 1]$, one has

$$-\boldsymbol{q}^T \widetilde{M}_i^j \boldsymbol{q} - \beta_1 < \boldsymbol{q}^T \widetilde{M}_i^j \boldsymbol{q} - 3\beta_1 < \boldsymbol{q}^T \widetilde{M}_i^j \boldsymbol{q} + \beta_1.$$

Hence the Hessian of V_q is positive definite and V_q is smooth and strictly convex. ■

IV. Controller Design

In this section, we derive a control law based on the logarithmic barrier potential function–now used as a Lyapunov function– defined in previous section. This will be achieved by observing that the spacecraft dynamics described by Eqs. (1)-(2) has a "cascaded" structure, thus making it suitable for control design based on the back-stepping method [15]. However, one of main drawback of a conventional back-stepping method is an embedded excessive control in the initial part of control signal and sluggish motion in the later part, that are not desirable in practical applications. In this direction, we adopt the modified back-stepping method [16] and propose an improved nonlinear error generation in the context of constrained attitude maneuver. First note that by letting

$$\dot{\boldsymbol{q}}(t) = -\nabla \boldsymbol{V}_q(\boldsymbol{q}),$$

we have

$$\dot{V}_q = \frac{\partial V_q}{\partial \boldsymbol{q}} \cdot \frac{\partial \boldsymbol{q}}{\partial t} = \nabla {V_q}^T \cdot \dot{\boldsymbol{q}} = -\|\nabla \boldsymbol{V}_q\|^2 < 0,$$

for all $\boldsymbol{q} \neq \boldsymbol{q}_r$, fulfilling the condition by V_q for being a *strong Lyapunov function* for the dynamics described by Eqs. (1)-(2) with respect to the equilibrium $\boldsymbol{q}_r$. In Eq. (1), we can consider $\widetilde{\boldsymbol{\omega}}$ as a "virtual" control input, making the system (1) asymptotically stable. In this direction, using quaternion identities we obtain

$$\widetilde{\boldsymbol{\omega}}_c = -2\boldsymbol{q}^\star \otimes \nabla \boldsymbol{V}_q. \tag{11}$$

Note that $\widetilde{\boldsymbol{\omega}}_c$ has the form of quaternion with the last element always zero as $\widetilde{\boldsymbol{\omega}}_c = [\ \vec{\omega}_c^T \quad 0\ ]^T$. Denote the error between $\widetilde{\boldsymbol{\omega}}$ and its desired value $\widetilde{\boldsymbol{\omega}}_c$ as,

$$\widetilde{\boldsymbol{z}} = \widetilde{\boldsymbol{\omega}} - \widetilde{\boldsymbol{\omega}}_c = \widetilde{\boldsymbol{\omega}} + 2\boldsymbol{q}^\star \otimes \nabla \boldsymbol{V}_q, \tag{12}$$

where $\widetilde{\boldsymbol{z}} = [\ \vec{z}^T \quad 0\ ]^T$. This error function $\widetilde{\boldsymbol{z}}$ acts as a feed-forward term and causes excessive control inputs in the initial part of the trajectory where the error magnitudes are the largest. Hence, we propose an improved error generation via as

$$\begin{aligned}\widetilde{\boldsymbol{z}} &= \alpha \arctan \beta(\widetilde{\boldsymbol{\omega}} - \widetilde{\boldsymbol{\omega}}_c) \\ &= \alpha \arctan \beta(\widetilde{\boldsymbol{\omega}} + 2\boldsymbol{q}^\star \otimes \nabla \boldsymbol{V}_q)\end{aligned} \tag{13}$$

where α and β are shaping parameters [16]. We can now obtain an equation for $\widetilde{\boldsymbol{\omega}}$ in $\widetilde{\boldsymbol{z}}$ as

$$\widetilde{\boldsymbol{\omega}} = \frac{1}{\beta} \tan\left(\frac{1}{\alpha} \widetilde{\boldsymbol{z}}\right) - 2\boldsymbol{q}^\star \otimes \nabla \boldsymbol{V}_q. \tag{14}$$

Next, by plugging $\widetilde{\boldsymbol{\omega}}$ into Eq. (1), we obtain the equation in terms of the error $\widetilde{\boldsymbol{z}}$:

$$\dot{\boldsymbol{q}} = \frac{1}{2} \boldsymbol{q} \otimes \left(\frac{1}{\beta} \tan\left(\frac{1}{\alpha} \widetilde{\boldsymbol{z}}\right)\right) - \nabla \boldsymbol{V}_q. \tag{15}$$

In addition, the time derivative of the vector part of Eq. (13) along with Eq. (2) is given by

$$\begin{aligned}J\dot{\vec{z}} &= J \frac{d}{dt} \alpha \arctan \beta(\vec{\omega} - \vec{\omega}_c) \\ &= C_1 \big(R(\omega)\, J\vec{\omega}(t) + \vec{u}(t) - J\dot{\vec{\omega}}_c\big),\end{aligned} \tag{16}$$

where $C_1 = \alpha\beta\big[I_3 + \beta^2 \mathrm{Diag}(\vec{\omega} - \vec{\omega}_c)^2\big]^{-1}$. In order to find an input $\vec{u}(t)$ which stabilizes the system (15)-(16), we define an augmented candidate Lyapunov function as

$$V(\boldsymbol{q}, z) = V_q + \frac{1}{2} \vec{z}^T J \vec{z}. \tag{17}$$

Taking the derivative of V (17) along the trajectories of Eqs. (15)-(16), we obtain,

$$\dot{V} = \nabla \boldsymbol{V}_q^T \left(\frac{1}{2} \boldsymbol{q} \otimes \widetilde{\boldsymbol{z}}\right) - \|\nabla \boldsymbol{V}_q\|^2 + \vec{z}^T C_1 (R(\omega)\, J\vec{\omega}(t) + \vec{u}(t) - J\dot{\vec{\omega}}_c). \tag{18}$$

By rearranging the term $\nabla \boldsymbol{V}_q^T (\frac{1}{2} \boldsymbol{q} \otimes \widetilde{\boldsymbol{z}})$ and using quaternion identities, Eq. (18) now yields,

$$\begin{aligned}\dot{V} = \vec{z}^T \big(&\frac{1}{2} q_0 \overrightarrow{\nabla V_q} + \frac{1}{2} \overrightarrow{\nabla V_q} \times \vec{q} - \frac{1}{2} \nabla V_{q0} \vec{q} + C_1 [R(\omega)\, J\vec{\omega}(t) \\ &+ \vec{u}(t) - J\dot{\vec{\omega}}_c]\big) - \|\nabla \boldsymbol{V}_q\|^2,\end{aligned} \tag{19}$$

where $\nabla \boldsymbol{V}_q = [\ \overrightarrow{\nabla V_q}^T \quad \nabla V_{q0}\ ]^T$. Thereby by choosing the actuator torque as,

$$\begin{aligned}\vec{u}(t) = J\dot{\vec{\omega}}_c - R(\omega)\, J\vec{\omega}(t) - C_1^{-1} \big[&\frac{1}{2} q_0 \overrightarrow{\nabla V_q} \\ &- \frac{1}{2} \overrightarrow{\nabla V_q} \times \vec{q} + \frac{1}{2} \nabla V_{q0} \vec{q} - \vec{z}\big],\end{aligned} \tag{20}$$

one has

$$\dot{V} = -\|\nabla \boldsymbol{V}_q\|^2 - \vec{z}^T \vec{z} \leq 0,$$

guaranteeing that the overall system is asymptotically stable. From Eq. (13), on the other hand, we note that

$$\vec{z} = \alpha \arctan \beta\big(\vec{\omega} - 2\nabla V_{q0} \vec{q} + 2q_0 \overrightarrow{\nabla V_q} - 2\vec{q} \times \overrightarrow{\nabla V_q}\big), \tag{21}$$

Now, rewriting the actuator torque $\vec{u}$ in $\vec{\omega}$ using the quaternion identities, we obtain,

$$\vec{u}(\vec{\omega}) = J\dot{\vec{\omega}}_c - R(\omega)\, J\vec{\omega} + \frac{1}{2} C_2 \overrightarrow{\nabla \boldsymbol{V}_q^\star \otimes \boldsymbol{q}} - \vec{z}, \tag{22}$$

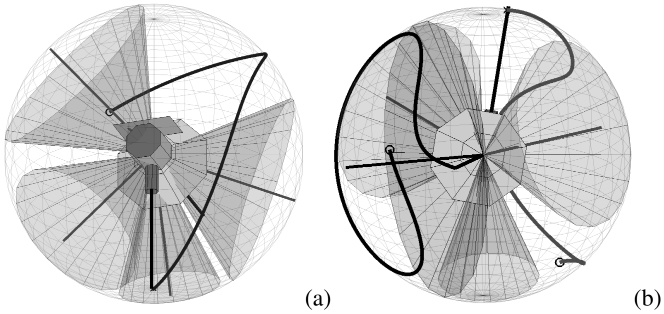

Fig. 4. Trajectory in the celestial attitude forbidden zone(a), and reorientation in the mandatory and forbidden zones(b).

where $\overrightarrow{\nabla \boldsymbol{V}_q^\star \otimes \boldsymbol{q}}$, consistent with the convention used in the paper, is the vector part of $\nabla \boldsymbol{V}_q^\star \otimes \boldsymbol{q}$, and $C_2 = (1/\alpha\beta)[I_3 + \beta^2 \mathrm{Diag}(\vec{\omega} - \vec{\omega}_c)^2]$.

The next step pertains to computing the term $\dot{\vec{\omega}}_c$ which appears in the control law Eq. (22). This term is the time derivative of Eq. (11), which should be computed directly when the control law is implemented. In the meantime, the time derivative of the vector part of $\widetilde{\boldsymbol{\omega}}_c$ can be given as,

$$\begin{aligned}\dot{\vec{\omega}}_c &= \frac{\partial}{\partial t}\big(2\nabla V_{q_0}\vec{q} - 2q_0\overrightarrow{\nabla V_q} + 2\vec{q}\times\overrightarrow{\nabla V_q}\big)\\ &= -2(\overrightarrow{\dot{\boldsymbol{q}}^\star \otimes \nabla \boldsymbol{V}_q + \boldsymbol{q}^\star \otimes \nabla^2 \boldsymbol{V}_q \dot{\boldsymbol{q}}}). \qquad (23)\end{aligned}$$

V. Simulation Results

In this section, we present simulation results for two types of attitude constrained scenarios. In simulations, it has been assumed that the spacecraft carries a light sensitive instrument with a fixed boresight in the spacecraft body axes, directed along the Z axis. Moreover, it is assumed that a high gain antenna has been mounted on the spacecraft such that its boresight is directed along the Y axis. We note that the parameters k_i in Eq. (8) influence the convergence rate of the algorithm as the corresponding logarithmic terms rapidly increase as the norm $\|\boldsymbol{q}_r^* \otimes \boldsymbol{q} - \boldsymbol{q}_{\mathbf{I}}\|^2$ associated with an attraction to the destination attitude decreases. From the simulations presented here, the values of k_i's are chosen around 0.005 for each constraint, while assuming the spacecraft's moments of inertia as,

$$J = \begin{bmatrix} 694 & 0 & 0 \\ 0 & 572 & 0 \\ 0 & 0 & 360 \end{bmatrix} (\mathrm{kg}\cdot m^2).$$

In general, larger values of k_i prolong the convergence to the destination attitude particularly when the desired attitude is in close proximity of the boundary of the constraint set.

Case 1: We consider the case in which the spacecraft is re-targeting its telescope from a randomly chosen initial attitude to a randomly chosen desired attitude, where both attitudes lie in the attitude permissible zone, satisfying the following inequalities for all i,

$$\boldsymbol{q}_0^T M_i^1 \boldsymbol{q}_0 < M0 \quad \text{and} \quad \boldsymbol{q}_r^T M_i^1 \boldsymbol{q}_r < 0,$$

where $\boldsymbol{q}_0$, $\boldsymbol{q}_r$ are an initial attitude and a desired attitude in unit quaternions, respectively. Also, we assume that there are four attitude forbidden zones in the spacecraft rotational configuration space. These zones are randomly chosen with the provision of not overlapping with each other. In Table I, the initial and desired spacecraft attitudes are given in unit quaternions as well as the

Initial Attitude (Case I)		Desired Attitude
[-0.188 -0.735 -0.450 -0.471]		[-0.59 0.67 0.21 -0.38]
Constraint object	**Angle**	**Type**
[0.174, -0.934, -0.034]	40 deg	Forbidden
[0, 0.7071 0.7071]	40 deg	Forbidden
[-0.853, 0.436, -0.286]	30 deg	Forbidden
[-0.122 -0.140 -0.983]	20 deg	Forbidden
Initial Attitude (Case II)		**Desired Attitude**
[0.714 0.637 -0.13 0.26]		[-0.23 0.008 0.491 -0.84]
Constraint object	**Angle**	**Type**
[0 -1 0]	40 deg	Forbidden
[0 0.8192 0.5736]	40 deg	Forbidden
[-0.8138 0.5483 -0.1926]	70 deg	Mandatory
[-0.122 -0.1397 -0.9827]	20 deg	Forbidden

TABLE I
SIMULATION PARAMETERS

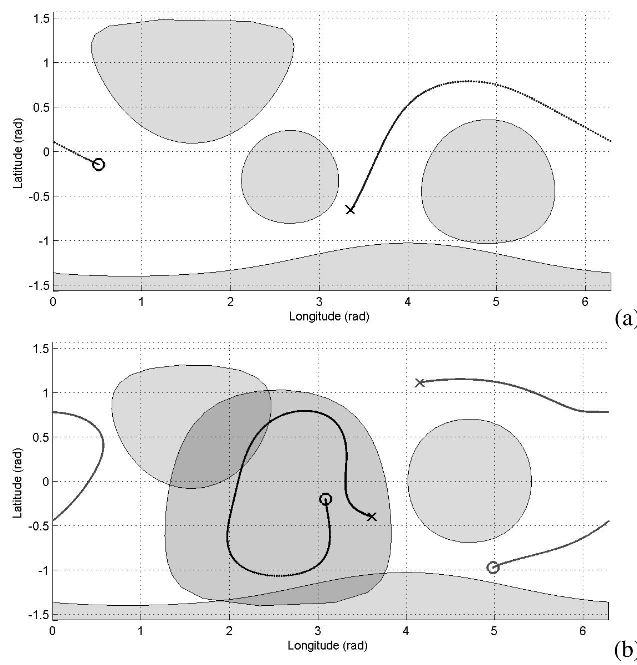

Fig. 5. Simulation trajectories on the 2-D cylindrical projection space

normalized position vectors, indicating four constrained sets (forbidden zones), all expressed with respect to the inertial frame. The simulation scenario has been conducted on these stationary initial attitudes. The potential function for this case is given as,

$$V_q(\boldsymbol{q}) = \|\boldsymbol{q}_r^\star \otimes \boldsymbol{q} - \boldsymbol{q}_{\mathrm{I}}\|^2 \Big[\Big(\sum_{i=1}^{4} -k_1 \log(-\frac{\boldsymbol{q}^T M_i^1 \boldsymbol{q}}{2})\Big)\Big],$$

where M_i^1 depends on the ith boresight vector indicating the constraint set. Fig. 4-a traces the pointing direction of the light sensitive instrument on the celestial sphere as well as the initial attitude ('$\circ$' mark) and the desired attitude ('$\times$' mark), while Fig. 5-a depicts the same trajectory as cylindrical projections of the corresponding celestial spheres. As shown in Fig. 6-a, the required final states are achieved asymptotically.

Case 2: In this case, we examine a reorientation maneuver for keeping a fixed boresight vector, e.g., an antenna, within a certain angle in order to continuously communicate with the ground station

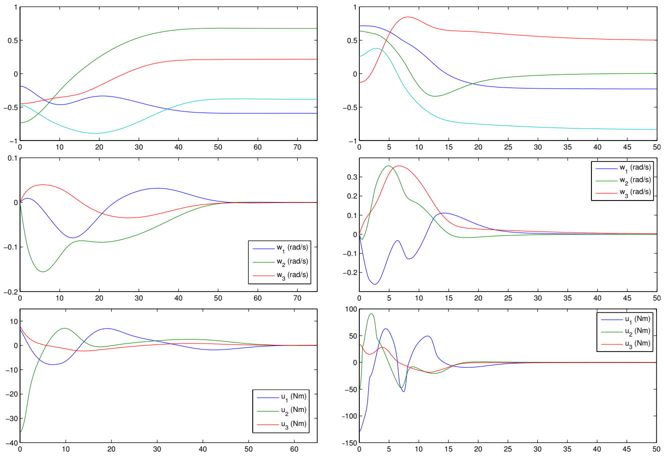

Case I (a) Case II (b)

Fig. 6. Simulation results–Quaternion trajectories, control inputs, and angular velocities over time (sec)

while the spacecraft is re-targeting its light sensitive instrument avoiding multiple bright objects or constrained zones. In this case, the feasible spacecraft attitude for reorientation can be represented using a combination of attitude mandatory zone and attitude forbidden zones. For this scenario, we have assumed that the antenna has been aligned along the Z-axis that the sensitive instrument has been aligned along the Y-axis, such that they their respective boresight vectors are perpendicular to each other; see Fig. 3. For the spacecraft reorientation to be feasible, the initial attitude $\boldsymbol{q}_0$ and desired attitude $\boldsymbol{q}_r$ should stay in the attitude permissible zone, where the following inequalities are satisfied,

$$\boldsymbol{q}_0^T M_M(\theta_M)\boldsymbol{q}_0 > 0 \quad \text{and} \quad \boldsymbol{q}_0^T M_i^j \boldsymbol{q}_0 < 0, \quad \forall\, i, j,$$

and

$$\boldsymbol{q}_r^T M_M(\theta_M)\boldsymbol{q}_r^T > 0 \quad \text{and} \quad \boldsymbol{q}_r^T M_i^j \boldsymbol{q}_r^T < 0, \quad \forall\, i, j.$$

The corresponding potential function is given as

$$V(\boldsymbol{q}) = \|\boldsymbol{q}_r^\star \otimes \boldsymbol{q} - \boldsymbol{q}_1\|^2 \Big[\Big(\sum_{i=1}^{3} -k_1 \log(-\frac{\boldsymbol{q}^T M_i^1 \boldsymbol{q}}{2}) \Big) - k_2 \log(\frac{\boldsymbol{q}^T M_M \boldsymbol{q}}{2}) \Big],$$

where M_1, M_2, and, M_3 are associated with the three attitude forbidden zones and M_M corresponds to the attitude mandatory zone. Fig. 4-a and 5-b demonstrate a reorientation maneuver while keeping the antenna's boresight vector within 70 deg permissible cone. The simulation parameters for this scenario are given in Table I. Fig. 6-b shows the quaternions trajectories, control inputs along the three independent spacecraft axes, as well as the spacecraft angular velocity, respectively.

VI. Conclusion

In this paper, an autonomous maneuver planning method for three axes attitude reorientation in presence of multiple types of attitude constraints has been proposed. This has been achieved via a logarithmic barrier potential that is built on the convex parameterization of attitude constraint sets in the quaternion space. Based on such a potential function, we then proceeded to embed a cascade form of spacecraft dynamics and kinematics that enabled us to obtain a controller by nonlinear back-stepping method. The main advantage of the proposed algorithm is its global convergence properties as well as its tractability and scalability for being implemented for distinct classes of attitude constraints. Since this approach is analytical and solvable with a minimum computational capability, it is attractive for on-board computation for slew maneuver planning.

Acknowledgments

The research of the authors has been supported by NSF Grant CMMI-0856737.

References

[1] McInnes, C., *Large Angle slew maneuvers with autonomous sun vector avoidance*, AIAA Journal of Guidance, Control and Dynamics, 17(4):875˜877, 1994.

[2] Wertz, J. R., *et al, Spacecraft Attitude Determination and Control*. Kluwer, Norwell, MA, 1978.

[3] McInnes, C., *Nonlinear control for large angel attitude slew maneuvers*, Proceedings of the Thirs ESA Symposium on Spacecraft Guidance, Navigation, and Control, pages 543-548. 1996.

[4] Spindler, K., *New Methods in On-board Attitude Control*, Advanced in the Astronautical Sciences, Vol. 100, No. 2, 1998, pp. 111-124.

[5] Hablani, H. B., *Attitude Commands Avoiding Bright Objects and Maintaining Communication with Ground Station*, Journal of Guidance, Control, and Dynamics, Vol. 22, No. 6, 1999, pp. 759-767.

[6] Frakes, J. P., Henretty, D. A., Flatley, T. W., Markley, F. L., San, J., and Lightsey, E. G., *SAMPEX Science Pointing with Velocity Avoidance*, in AAS/AIAA Spaceflight Mechanics Meeting, Colorado Springs, CO, 1992, pp. 949-966.

[7] Frazzoli, E., Dahleh, M. A., Feron, E., Kornfeld, R. P., *A randomized Attitude Slew Planning Algorithm for Autonomous Spacecraft*, AIAA Journal of Guidance, Control and Dynamics, 2001.

[8] Wie, B., and Barba, P.M., *Quaternion Feedback for Spacecraft Large Angle Maneuvers*, Journal of Guidance, Control and Dynamics, Vol. 8, No. 3, 1985 pp. 360-365.

[9] Cui, P., Zhong, W., Cui, H., *Onboard Spacecraft Slew-Planning by Heuristic State-Space Search and Optimization*, 2007 International Conference on Mechatronics and Automation. 2007: 2115-2119.

[10] Ahmed, A., Alexander, J., Boussalis, D., Breckenridge, W., Macala, G., Mesbahi, M., San Martin, M., Singh, G., and Wong, E., *Cassini Control Analysis Book*, Jet Propulsion Laboratory, 1998.

[11] Kornfeld, .R. P., *On-board Autonomous Attitude Maneuver Planning for Planetary Spacecraft using Genetic Algorithms*, AIAA Conf. on Guidance, Navigation and Control, 2003.

[12] Kim Y., Mesbahi M., Singh G, Hadaegh F., *On the Convex Parametrization of Spacecraft Orientation in Presence of Constraints and its Applications*, AIAA. 2006.

[13] Kim Y., Mesbahi M., *Quadratically Constrained Attitude Control via Semidefinite Programming*, IEEE Transactions on Automatic Control. 2004.

[14] Tsiotras, M. P., Corless, M., and Longuski, J. M., *Novel Approach to the Attitude Control of Axi-Symmetric Spacecraft*, Automatica, Vol. 31, No. 8, pp.1099-1112, 1995.

[15] Freeman, R. A., and P. Kokotović, *Robust Nonlinear Control Design: State Space and Lyapunov Techniques*, Birkhuser, 1996.

[16] Kim, K., Kim, Y., Robust Backstepping Control for Slew Maneuver Using Nonlinear Tracking Function, IEEE Transactions on Control Systems Technology, Vol. 11, No. 6, 2003